Journal of Computer Science and Artificial Intelligence
ISSN: 3078-8242 (Print), ISSN: 3078-2309 (Online) | Vol. 8, No. 1, 2026

A Review of Recent Advances in Control Algorithms for Stewart Platforms

Hemin Zhang, Lin Wang

School of Navigation of Shipping, Shandong Jiaotong University, Weihai 264209, Shandong, People's Republic of China

Abstract: The Stewart platform is a typical six-degree-of-freedom parallel mechanism characterized by high load-carrying capacity, high structural stiffness, a short error propagation chain, and fast dynamic response. It has been widely used in motion simulation, ship motion compensation, space payload pointing, precision machining, and multidimensional vibration control. Because the moving platform is cooperatively driven by six kinematic chains, its control system exhibits pronounced nonlinearity, strong coupling, and multivariable characteristics, and is affected by factors such as mechanical clearance, load variations, actuator saturation, sensor noise, and model parameter errors. Although conventional proportional-integral-derivative (PID) control has a simple structure and is easy to implement in engineering applications, it often struggles to simultaneously achieve high tracking accuracy, fast response, and stable operation under complex attitude variations and persistent external disturbances. In recent years, methods such as model predictive control, sliding mode control, adaptive control, robust control, neural networks, and reinforcement learning have gradually been introduced into Stewart platform systems. This review examines recent control strategies for Stewart platforms against four practical criteria: model requirements, disturbance rejection, constraint handling, and computational demand. The discussion also covers the validation methods and application conditions reported in marine compensation, motion simulation, aerospace positioning, precision machining, and vibration isolation. Particular attention is given to unresolved issues in modeling accuracy, sensing delay, real-time implementation, safety, and the generalization of learning-based controllers.

Keywords: Stewart platform, parallel robot, motion control, model predictive control, sliding mode control, neural network, wave-induced motion compensation.

1. Introduction

The Stewart platform typically consists of a fixed base, a moving platform, and six independently extensible legs. Through coordinated adjustment of the leg lengths, the moving platform can produce translations along three axes and rotations about three axes. Because the external load is shared by multiple legs, this parallel mechanism offers a favorable combination of high structural stiffness, large load-carrying capacity, and fast dynamic response. With advances in servo actuation, sensing and measurement, and real-time computing technologies, its applications have gradually expanded beyond conventional flight simulators to marine equipment, space-based optical systems, intelligent manufacturing, and multi-degree-of-freedom vibration isolation. Wang et al. reviewed the configurations, actuation modes, and application areas of Stewart parallel robots and noted that high-precision pose control and multi-degree-of-freedom vibration suppression have become major research directions in this field [1].

The parallel architecture of the Stewart platform shortens the error propagation chain but also introduces strong coupling among the legs. A change in any pose component of the moving platform generally requires coordinated adjustment of multiple legs, and a positioning error in a single leg may be mapped into several spatial degrees of freedom. Liang et al. analyzed platform pose resolution in terms of leg displacement increments and showed that actuator resolution and joint arrangement jointly affect the final motion accuracy [2]. From a kinematic perspective, the inverse solution generally provides the six leg lengths directly from a prescribed pose, whereas the forward solution determines the moving-platform pose from the leg lengths and therefore involves a set of multivariable nonlinear equations. Xie et al. formulated the forward kinematics as an iterative optimization problem on the Lie group SE(3), offering a new approach to improving convergence [3]. Forward kinematics is relevant not only to pose feedback but also to parameter calibration, error compensation, and state estimation. Platform geometry likewise affects control performance. Fang et al. used parametric modeling to analyze how structural dimensions and joint layout influence the workspace and motion performance, showing that design parameters are closely related to the achievable attitude range and dynamic performance of the controller [4]. In addition to pose regulation, Stewart mechanisms have also been applied to low-frequency vibration isolation and energy management. Lu et al. introduced high-static-low-dynamic-stiffness characteristics into a parallel platform, thereby reducing the onset frequency of vibration isolation while maintaining load capacity, and further investigated the integrated design of vibration isolation and energy harvesting [5].

The achievable control performance is determined not only by servo tuning, but also by mechanism geometry, kinematic accuracy, dynamic uncertainty, state estimation, actuator limits, and the available computation time.

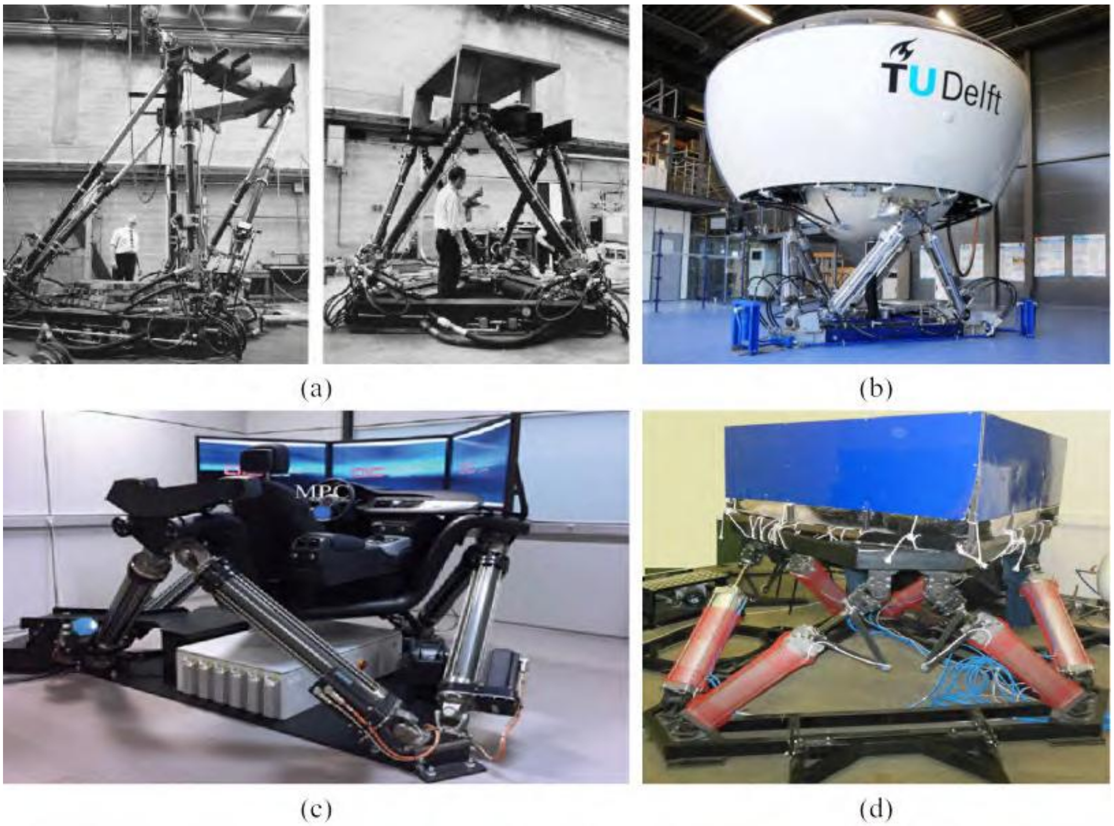

Figure 1. (a) The world's first six-degree-of-freedom flight simulator [29]; (b) the Simona flight simulator [30]; (c) a driving simulator [7]; and (d) a driving test simulator [31].

2. Mathematical Model

To model a Stewart platform, a base coordinate frame $\{B\}$ is generally established at the center of the fixed platform, and a moving coordinate frame $\{P\}$ at the center of the moving platform. Let the position of the i-th joint on the fixed platform in the base frame be b_i, the position of the corresponding joint on the moving platform in the moving frame be p_i, and the position vector of the moving-platform center be:

$$\mathrm{r} = [x, y, z]^T \tag{1}$$

The platform attitude is described by the roll angle ϕ, pitch angle θ, and yaw angle ψ, and the rotation matrix can be written as:

$$\mathrm{R} = \mathrm{R}_z(\psi)\mathrm{R}_y(\theta)\mathrm{R}_x(\phi) \tag{2}$$

The spatial vector of the i-th leg is:

$$\mathrm{l}_i = \mathrm{r} + \mathrm{R}\mathrm{p}_i - \mathrm{b}_i \tag{3}$$

The corresponding leg length is:

$$L_i = \| \mathrm{l}_i \| \tag{4}$$

Combining the lengths of the six legs gives the inverse kinematic relationship:

$$\mathrm{L} = f(\mathrm{X}) \tag{5}$$

Where:

$$\mathrm{L} = [L_1, L_2, L_3, L_4, L_5, L_6]^T \tag{6}$$

$$\mathrm{X} = [x, y, z, \phi, \theta, \psi]^T \tag{7}$$

Inverse kinematics is a fundamental component of real-time platform control. The controller first generates the desired position and attitude, converts them into target lengths for the six legs, and then commands the actuators to track these targets. Differentiating the leg-length equations yields the mapping between the generalized velocity of the platform and the leg velocities:

$$\dot{\mathrm{L}} = \mathrm{J}(\mathrm{X})\dot{\mathrm{X}} \tag{8}$$

Where J is the Jacobian matrix. It determines the velocity mapping and also describes the transmission of leg forces to the generalized forces acting on the platform:

$$\tau = \mathrm{J}^T \mathrm{f} \tag{9}$$

When the Jacobian matrix approaches rank deficiency, the platform enters a near-singular state. In this condition, a small pose variation may require large leg velocities or driving forces, which can lead to actuator saturation, increased tracking error, or even system instability. Trajectory planning should therefore consider not only whether the desired pose lies within the geometric workspace, but also the Jacobian condition number, joint-angle limits, and the remaining actuator stroke. The platform dynamics can be derived using the Lagrange method, the Newton-Euler method, or the principle of virtual work, and can generally be expressed as:

$$\mathrm{M}(\mathrm{X})\ddot{\mathrm{X}} + \mathrm{C}(\mathrm{X}, \dot{\mathrm{X}})\dot{\mathrm{X}} + \mathrm{G}(\mathrm{X}) + \mathrm{F}_f(\dot{\mathrm{X}}) + \mathrm{d}(t) = \mathrm{J}^T(\mathrm{X}) \tag{10}$$

Where M is the mass matrix, C contains the Coriolis and centrifugal terms, G is the gravity term, F_f represents friction, clearance, and actuator nonlinearities, and $d(t)$ denotes the external disturbance. If leg mass, ball-screw inertia, payload-center-of-mass offset, and structural flexibility are further considered, the model accuracy can be improved, although the online computational burden also increases. Zhang et al. jointly optimized the structural parameters and effective workspace of a driving-simulator platform, showing that the mechanically reachable range should be matched to the control task during the design stage [6].

Engineering systems commonly adopt a hierarchical modeling framework. A simplified servo model is used at the lower level, inverse kinematics is used at the intermediate level to allocate leg commands, and dynamic feedforward compensation, disturbance observation, or constrained optimization is introduced at the upper level as required by the task. This approach retains the dominant coupling relationships while avoiding the excessive computational burden of a complete nonlinear dynamic model. After selecting the state variables and discretizing the model, the platform dynamics can be written as:

$$\mathrm{x}_{k+1} = \mathrm{A}_k \mathrm{x}_k + \mathrm{B}_k \mathrm{u}_k + \mathrm{E}_k \mathrm{d}_k \tag{11}$$

During operation, the platform is generally subject to constraints on leg length, velocity, and acceleration:

$$\begin{aligned} L_{i,\min} &\leq L_i \leq L_{i,\max} \\ |\dot{L}_i| &\leq \dot{L}_{i,\max} \\ |\ddot{L}_i| &\leq \ddot{L}_{i,\max} \end{aligned} \tag{12}$$

In wave-motion compensation and attitude stabilization systems, tilt sensors or inertial measurement units (IMUs) are commonly used to measure the platform attitude. The measured signals contain noise, zero drift, installation misalignment, and communication delay. Although filtering can suppress high-frequency fluctuations, it also introduces phase lag. If the filter delay approaches the platform control period, the compensation action may lag behind the disturbance variation and cause repeated tilting. Sensor processing must therefore balance signal smoothing against closed-loop dynamic response.

3. Review and Comparison of Mainstream Control Algorithms

3.1. Basic Feedback, Adaptive, and Robust Control

PID control is the most widely used basic control method for Stewart platforms. The desired pose is generally converted through inverse kinematics, after which independent position loops are established for the six legs:

$$u_i(t) = K_{pi} e_i(t) + K_{ii} \int_0^t e_i(\tau)\, \mathrm{d}\tau + K_{di} \frac{\mathrm{d}e_i(t)}{\mathrm{d}t} \tag{13}$$

PID control does not require a complex dynamic model, has a low computational burden, and can be readily implemented on motion controllers, programmable logic controllers, and servo drives. When the platform operates over a limited range and the load variation is small, appropriate tuning can provide stable tracking performance. Santos Arconada et al. investigated ride-comfort simulation on an electric Stewart platform and improved the platform response within a specified frequency range through motion planning and closed-loop control [7]. The main limitation of conventional PID control is that its gains are fixed and the legs are usually approximated as independent channels. When the platform performs coupled attitude motions or the payload changes, the original gains may no longer be suitable. An excessively low proportional gain leads to insufficient compensation, whereas an excessively high gain may cause overshoot. Integral action reduces steady-state error but may accumulate excessively under actuator saturation. Li et al. proposed a BP-neural-network-based PID method for a shipborne platform, in which the network adjusts the controller gains online according to the error state, thereby reducing the position deviation under wave disturbances [8].

Adaptive control updates model or controller parameters online so that the system can accommodate variations in payload, friction, and actuator characteristics. Yi et al. developed a control architecture for a magnetostrictive Stewart platform that combines hysteresis compensation, adaptive feedforward control, and PID feedback. An adaptive filter was used to learn periodic disturbances, enabling coordinated micropositioning and vibration suppression [9]. Fuzzy control adjusts the control gains according to the tracking error and its rate of change and therefore does not require a highly accurate dynamic model. Ma et al. applied optimized fuzzy control to a cubic Stewart seat suspension and improved the vibration responses in the vertical, horizontal, and roll directions [10]. Adaptive and fuzzy methods improve operating-condition adaptability, but overly rapid parameter updates may amplify sensor noise, whereas slow updates cause adaptation lag. In engineering applications, these methods are therefore commonly used as gain-adjustment layers for PID control rather than as complete replacements for the lower-level feedback loop.

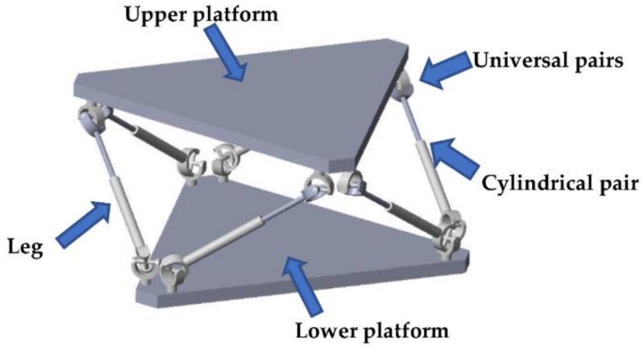

Figure 2. Structure of the cubic Stewart seat suspension [10].

Sliding mode control constructs a sliding surface so that the system error approaches the desired trajectory within a finite time. Let the pose error be e; the sliding variable can then be defined as:

$$\mathrm{s} = \dot{\mathrm{e}} + \Lambda \mathrm{e} \tag{14}$$

This method is strongly robust to parameter perturbations and external disturbances. Chen et al. addressed the attitude-tracking problem of a satellite with flexible appendages by combining nonsingular terminal sliding mode control with a control Lyapunov function to accelerate attitude-error convergence [11]. However, the switching term in conventional sliding mode control may cause high-frequency chattering, which can appear on a physical platform as frequent actuator reversals and mechanical impacts. Saturation functions, higher-order sliding modes, or disturbance observers are therefore often introduced to alleviate this problem.

Robust control places greater emphasis on maintaining closed-loop stability in the presence of bounded parameter uncertainty. Dong et al. established a dynamic model of a Stewart-platform satellite that accounts for flexible solar panels and investigated integrated attitude-pointing control, demonstrating that coupling between the flexible appendages and platform motion can significantly affect the system dynamics [12]. Du et al. developed a comprehensive parametric model for a large spaceborne optical payload and reduced the coupling among multiple degrees of freedom through parameter matching and decoupling design [13]. Robust methods provide strong disturbance rejection, but an overly conservative uncertainty bound may lead to excessive control action, whereas an underestimated bound may fail to cover the actual operating conditions.

3.2. Model Predictive Control and Intelligent Control

At each sampling instant, model predictive control predicts the future platform motion over a finite horizon from the current state and calculates the control input through receding-horizon optimization. A typical objective function is:

$$J = \sum_{j=1}^{N_p} \left\| \mathrm{y}_{k+j|k} - \mathrm{y}_{d,k+j} \right\|_{\mathrm{Q}}^{2} + \sum_{j=0}^{N_c-1} \left\| \Delta \mathrm{u}_{k+j|k} \right\|_{\mathrm{R}}^{2} \quad (15)$$

Where N_p is the prediction horizon, N_c is the control horizon, and Q and R weight the tracking error and the variation in control input, respectively. Zhao et al. proposed a switchable MPC strategy that uses a higher-accuracy predictive mode when the platform is far from the boundary and switches the control formulation near the constraint boundary to reduce the risk of optimization infeasibility [14]. Chadha et al. developed a hybrid method in which explicit MPC supplies a warm-start initial value for implicit MPC, thereby reducing the online computational burden of motion cueing for driving simulators [15]. MPC can directly handle constraints on leg stroke, velocity, acceleration, and platform attitude and is therefore well suited to coordinated multi-degree-of-freedom control. However, its performance depends on the prediction model, and its online computational cost is substantially higher than that of PID or sliding mode control. Increasing the tracking weight accelerates the response but may cause overly rapid changes in the leg commands, whereas increasing the control-increment weight suppresses oscillation at the expense of slower compensation. The parameters should therefore be selected jointly according to actuator bandwidth, sampling period, and disturbance frequency.

Neural networks are mainly used for forward-kinematics solution, parameter adjustment, model-error compensation, and control-policy approximation in Stewart platforms. Zhu et al. represented the relationships among the platform joints and legs using a distance graph neural network and combined the network with numerical iteration to improve the accuracy of the forward-kinematics solution, providing a new approach to real-time pose estimation [16]. Maldonado et al. integrated visual detection with platform attitude control and adjusted the platform inclination to move a ball toward a target position, demonstrating the potential of parallel platforms in dynamic interaction tasks [17]. Reinforcement learning obtains a control policy through interaction between an agent and its environment. Scheidel et al. used proximal policy optimization to learn a motion-cueing strategy for a general motion simulator and balanced workspace utilization against human motion-perception error [18]. Gonzalez Arango et al. used a policy network to approximate a nonlinear model predictive controller for a serial-robot motion simulator, moving most of the optimization computation to offline training and providing a useful reference for real-time learning-based MPC on parallel platforms [19]. Ketchum et al. established a machine-learning-based kinematic mapping for a soft Stewart platform and combined it with PID control to perform dynamic balancing tasks [20]. Avtges et al. further investigated the ability of reinforcement learning to recover control policies on a soft parallel platform after actuator performance degradation [21].

Data-driven methods have strong approximation capabilities for friction, hysteresis, and complex nonlinearities, but their performance depends on the training data, and large errors may occur outside the training range. Industrial platforms are therefore better suited to a framework in which the physical model provides the main control structure and the learning model supplies compensation. In this framework, the network performs model correction, MPC acceleration, or parameter tuning, while a controller with verified stability manages the lower-level closed loop. State estimation and safety constraints are also essential for applying advanced controllers to physical platforms. Cinun et al. combined an extended Kalman filter with nonlinear control and fused IMU measurements with actuator feedback to improve state estimation on a low-cost platform [22]. The same group subsequently investigated control-barrier-function-based safety control, reducing the online optimization burden while satisfying multiple position and velocity constraints [23].

3.3. Overall Comparison of Control Algorithms

Table 1. Comparison of the main control methods for Stewart platforms

Control method	Disturbance rejection	Constraint handling	Real-time performance	Main advantages	Main limitations
PID	Moderate	Limited	High	Simple structure and mature implementation	Difficult to handle strong coupling and parameter variations
Fuzzy/neural-network PID	Relatively strong	Limited	Relatively high	Online gain adjustment	Complex rule design or training process
Adaptive control	Relatively strong	Moderate	Relatively high	Adapts to parameter variations	Sensitive to noise and adaptation laws
Sliding mode control	Strong	Moderate	High	Fast convergence and strong robustness	Possible chattering
Robust control	Strong	Moderate	Relatively high	Well-established stability theory	Potentially conservative design
MPC	Relatively strong	Strong	Moderate	Prediction and explicit constraint handling	High online computational cost
Neural networks and reinforcement learning	Depends on training	Can be incorporated during training	Fast inference	Strong nonlinear learning capability	Limited generalization and interpretability

No single controller dominates across all operating conditions. Low-level servo loops favor computationally inexpensive feedback laws, whereas platform-level coordination benefits from model-based coupling compensation and explicit constraint handling. Learning-based methods are most useful when they complement, rather than replace, a verified feedback structure. The practical choice is therefore governed by the required bandwidth, model uncertainty, available sensing, and computational resources.

4. Simulation and Experimental Validation and Application Scenarios

4.1. Simulation and Experimental Validation

The reviewed studies use three main levels of validation. MATLAB/Simulink is commonly used for initial controller assessment, whereas ADAMS or Simscape Multibody is introduced when leg forces, joint limits, and structural interference must be represented. Hardware tests are less common, but they are essential for revealing effects that are absent from idealized models, particularly sensor delay, servo bandwidth, friction, and actuator saturation.

Coupled multibody-dynamics simulation commonly uses ADAMS or Simscape Multibody to construct the mechanical model and exchange data with the controller. This method allows leg forces, joint-motion ranges, and structural interference to be examined and is suitable for validating large-range coupled motions. Physical experiments must additionally consider the motion-controller cycle, bus communication, internal servo-drive control, encoder resolution, and sensor delay. A comprehensive validation program should include single-degree-of-freedom motion, multi-degree-of-freedom composite trajectories, payload variations, external disturbances, and long-duration operation. In addition to root-mean-square error, the reported metrics should include maximum error, overshoot, settling time, peak control input, leg-stroke utilization, and computation time per control cycle. Vibration-isolation studies should also report transmissibility and frequency-domain attenuation, whereas motion-simulation studies should evaluate perceptual error and workspace utilization.

4.2. Typical Application Scenarios

Marine applications mainly include motion reproduction and wave-motion compensation. In a wave-motion compensation system, a tilt sensor or IMU measures the platform attitude, the controller calculates the difference between the desired horizontal attitude and the measured attitude, and inverse kinematics distributes the compensation command among the six legs. This process is sensitive to sensor noise, filter delay, compensation direction, and actuator saturation. Excessive filtering causes the platform response to lag behind the wave motion, whereas an overly high gain may produce a repeated sequence of tilting, overcompensation, and reverse tilting. Wave-motion compensation should therefore adopt a hierarchical architecture that combines an attitude outer loop, leg-position inner loops, state observation, and constraint management.

In aerospace and precision-pointing applications, Stewart platforms are mainly used for mirror adjustment, payload pointing, and microvibration suppression. Kazezkhan et al. optimized a modified platform for a large radio telescope to improve stiffness and load distribution at different elevation angles [24]. Liang et al. developed a high-precision Stewart platform for a space camera and evaluated its translational and angular resolution [25]. Such tasks generally involve a small motion range but impose stringent requirements on repeatability, low-speed stability, and microvibration control. For multi-degree-of-freedom vibration isolation, Sun et al. analyzed the nonlinear coupled vibration of a quasi-zero-stiffness Gough-Stewart platform and showed that the system may exhibit multiple equilibrium positions and jump responses, while excitation in different directions can also change the coupling state [26]. These findings indicate that the six degrees of freedom cannot simply be treated as fully independent in vibration-isolation control. To balance load capacity and low-frequency isolation performance, recent studies have increasingly combined quasi-zero-stiffness or negative-stiffness mechanisms, piezoelectric actuators, or magnetorheological dampers with active control.

In precision machining, a Stewart mechanism can serve as the core motion unit of a parallel machine tool. In addition to pose tracking, the controller must account for cutting loads, variations in structural stiffness, and geometric-error compensation. Pu et al. analyzed and optimized the workspace, motion performance, and structural parameters of a 6-UPS parallel machine tool [27]. Future systems may use force sensing, visual measurement, and digital-twin models to estimate cutting loads and correct tool trajectories.

Table 2. Typical applications and control requirements of Stewart platforms

Application scenario	Primary objective	Applicable control methods	Main performance metrics
Ship-motion reproduction	Reproduce roll, pitch, and heave	PID, feedforward control, and MPC	Pose error and frequency consistency
Shipborne wave-motion compensation	Stabilize the upper platform	ADRC, sliding mode control, and MPC	Residual attitude and settling time
Flight and driving simulation	Reproduce motion perception	Washout algorithms, MPC, and learning-based control	Perceptual error and workspace utilization
Space-payload pointing	High-precision attitude adjustment	Robust, sliding mode, and feedforward control	Pointing error and stability
Multi-degree-of-freedom vibration isolation	Reduce vibration transmission	Adaptive and active vibration control	Transmissibility and resonance peak
Parallel machine tools	Generate spatial machining trajectories	Feedforward, robust, and error-compensation control	Contour error and machining accuracy

5. Current Challenges and Future Research Directions

Despite recent advances, several factors still limit the transfer of Stewart platform control methods from simulation to physical systems. Most analytical models assume rigid links, ideal joints, accurate geometric parameters, and fixed payload properties, whereas practical platforms are affected by friction, joint clearance, structural flexibility, payload variation, and installation errors. Simplified models may therefore fail to describe the actual system dynamics, while highly detailed models increase the computational burden of real-time control. Calibration is subject to a similar limitation. Errors in joint coordinates, initial leg lengths, and sensor installation angles can lead to noticeable pose deviations. Karmakar and Turner noted that current calibration studies mainly focus on kinematic and structural errors, while environmental effects and loaded operating conditions receive less attention [28]. In addition, advanced algorithms such as nonlinear MPC and high-order state observers may require more computation than an industrial controller can provide within one sampling period.

Sensing, filtering, and safety constraints also remain important practical issues. Tilt sensors provide stable low-frequency attitude information, whereas gyroscopes offer faster angular-rate measurements but are affected by drift. Excessive filtering can suppress noise but may also introduce phase lag, especially in shipborne compensation systems subjected to continuously changing wave-induced motion. At the same time, leg stroke, actuator velocity, joint-angle limits, and proximity to singular configurations must be considered during coordinated motion. Simple command saturation is easy to implement, but it may distort the desired platform motion and increase coupling among the legs. These limitations suggest that future systems should adopt hierarchical control architectures. Fast PID or state-feedback loops can be retained at the actuator level, while platform-level controllers handle coupling compensation and attitude regulation, and a supervisory MPC layer manages workspace and safety constraints. State estimation based on IMU, tilt-sensor, encoder, or vision measurements can further improve feedback quality.

For systems affected by uncertain payloads, friction, or external disturbances, a practical approach is to combine a reduced-order physical model with disturbance observers or learning-based residual compensation. Neural networks may support forward-kinematics estimation, parameter adaptation, or rapid approximation of optimization-based controllers, but they should operate within verified physical and safety constraints. In shipborne applications, sensor fusion, disturbance estimation, short-term prediction, an attitude outer loop, and leg-position inner loops can be integrated into a unified framework. Such an arrangement is more suitable than directly negating the measured attitude and applying it to inverse kinematics. Future studies should also adopt more consistent validation procedures and report not only root-mean-square error, but also maximum error, overshoot, settling time, actuator demand, leg-stroke utilization, computation time, and frequency-dependent compensation performance.

6. Conclusions

The Stewart platform provides high stiffness, large load capacity, and flexible six-degree-of-freedom motion, but its parallel architecture also introduces strong coupling, nonlinear dynamics, workspace constraints, and sensitivity to geometric and sensing errors. The reviewed studies show that PID control remains suitable for actuator inner loops because of its simplicity and real-time performance, whereas adaptive, fuzzy, sliding mode, and robust control improve disturbance rejection and parameter adaptability. MPC is particularly useful when actuator and workspace constraints must be handled explicitly. Neural networks and reinforcement learning offer additional tools for nonlinear modeling and controller approximation, although their practical use still depends on training coverage, computational resources, and safety supervision.

No single algorithm is suitable for all Stewart platform applications. Precision positioning emphasizes calibration accuracy, motion simulators require efficient workspace utilization, vibration-isolation systems focus on frequency-domain performance, and shipborne platforms must respond continuously to uncertain motion. A hierarchical hybrid architecture is therefore a promising engineering solution: reliable servo loops ensure actuator-level stability, state estimation and disturbance compensation improve platform-level performance, and predictive optimization manages workspace and safety constraints. Further progress will depend on the coordinated development of mechanical design, sensing, modeling, calibration, and control, together with more extensive experimental validation under realistic operating conditions.

References

[1] Wang, M., Zhang, Y., Liang, Q., et al. (2025). Development status and frontier applications of Stewart parallel intelligent robots. Chinese Journal of Nature, 47(5), 360–372. https://doi.org/10.3969/j.issn.0253-9608.2025.05.004 (In Chinese)

[2] Liang, F. C., Zhao, X. L., Tan, S., et al. (2022). Pose resolution analysis method for a Stewart six-degree-of-freedom parallel mechanism. Journal of Changchun University of Science and Technology (Natural Science Edition), 45(6), 110–117. https://doi.org/10.3969/j.issn.1672-9870.2022.06.017 (In Chinese)

[3] Xie, B., Dai, S., & Liu, F. (2021). A Lie group-based iterative algorithm framework for numerically solving forward kinematics of Gough-Stewart platform. Mathematics, 9(7), 757. https://doi.org/10.3390/math9070757

[4] Fang, X. G., Zhang, W., Zheng, M. L., et al. (2021). Parametric modeling and optimization of a six-degree-of-freedom Stewart platform. Journal of Harbin University of Science and Technology, 26(1), 66–76. https://doi.org/10.15938/j.jhust.2021.01.010 (In Chinese)

[5] Lu, Z. Q., Wu, D., Ding, H., et al. (2021). Vibration isolation and energy harvesting integrated in a Stewart platform with high static and low dynamic stiffness. Applied Mathematical Modelling, 89, 249–267. https://doi.org/10.1016/j.apm.2020.07.060

[6] Zhang, T. T., Zhao, X., Ni, X., et al. (2021). Development and optimization of a six-degree-of-freedom Stewart platform for driving simulation devices. Industrial Technology Innovation, 8(5), 109–113. https://doi.org/10.14103/j.issn.2095-8412.2021.10.019 (In Chinese)

[7] Santos Arconada, V., García-Barruetabeña, J., & Haas, R. (2023). Validation of a ride comfort simulation strategy on an electric Stewart platform for real road driving applications. Journal of Low Frequency Noise, Vibration and Active Control, 42(1), 368–391. https://doi.org/10.1177/14613484221122109

[8] Li, D., Wang, S., Song, X., et al. (2024). A BP-neural-network-based PID control algorithm of shipborne Stewart platform for wave compensation. Journal of Marine Science and Engineering, 12(12), 2160. https://doi.org/10.3390/jmse12122160

[9] Yi, S., Zhang, Q., Sun, X., et al. (2023). Simultaneous micropositioning and microvibration control of a magnetostrictive Stewart platform with synthesized strategy. Mechanical Systems and Signal Processing, 187, 109925. https://doi.org/10.1016/j.ymssp.2022.109925

[10] Ma, T., Li, T., Jing, G., et al. (2022). Development of a novel seat suspension based on the cubic Stewart parallel mechanism and magnetorheological fluid damper. Applied Sciences, 12(22), 11437. https://doi.org/10.3390/app122211437

[11] Chen, X., Zhu, H., Yin, J., et al. (2023). A NTSMCLF attitude tracking controller for the satellite with flexible accessories based on the Stewart platform. In Proceedings of the 42nd Chinese Control Conference (pp. 3006–3011). IEEE. https://doi.org/10.23919/ccc58697.2023.10239867

[12] Dong, A. L., Lyu, L. L., Cai, G. P., et al. (2022). Dynamics modeling and integrated attitude pointing control of a Stewart platform satellite. Chinese Space Science and Technology, 42(6), 79–88. (In Chinese)

[13] Du, L., Luo, Y., Ji, L., et al. (2025). Comprehensive parametric model and decoupling design of a Stewart platform for a large spaceborne optical load. Acta Astronautica, 226, 119–134. https://doi.org/10.1016/j.actaastro.2024.11.036

[14] Zhao, J., Xu, Z., Wu, D., et al. (2025). Six-DoF Stewart platform motion simulator control using switchable model predictive control. arXiv:2503.11300. https://doi.org/10.48550/arXiv.2503.11300

[15] Chadha, A., Jain, V., Rios Lazcano, A. M., et al. (2023). Computationally-efficient motion cueing algorithm via model predictive control. arXiv:2304.03232. https://doi.org/10.48550/arXiv.2304.03232

[16] Zhu, H., Xu, W., Huang, J., et al. (2024). DisGNet: A distance graph neural network for forward kinematics learning of Gough-Stewart platform. arXiv:2402.09077. https://doi.org/10.48550/arXiv.2402.09077

[17] Maldonado, A., Bueno, C., Loza, D., et al. (2021). Design, construction and implementation of Stewart platform with control of rolling ball on platform through artificial vision. arXiv:2105.10963. https://doi.org/10.48550/arXiv.2105.10963

[18] Scheidel, H., Asadi, H., Bellmann, T., et al. (2024). A deep reinforcement learning based motion cueing algorithm for vehicle driving simulation. IEEE Transactions on Vehicular Technology, 73(7), 9696–9705. https://doi.org/10.1109/TVT.2024.3375941

[19] Gonzalez Arango, C., Asadi, H., Chalak Qazani, M. R., et al. (2025). Learning-based approximate nonlinear model predictive control motion cueing. arXiv:2504.00469. https://doi.org/10.48550/arXiv.2504.00469

[20] Ketchum, J., Avtges, J., Schlafly, M., et al. (2025). Force and speed in a soft Stewart platform. arXiv:2504.13127. https://doi.org/10.48550/arXiv.2504.13127

[21] Avtges, J., Ketchum, J., Schlafly, M., et al. (2025). Real-time reinforcement learning for dynamic tasks with a parallel soft robot. In 2025 IEEE/RSJ International Conference on Intelligent Robots and Systems (IROS) (pp. 5537–5544). IEEE. https://doi.org/10.1109/IROS60139.2025.11246440

[22] Cinun, B. C. G., Tamba, T. A., Santjoko, I. R., et al. (2025). End-to-end design and validation of a low-cost Stewart platform with nonlinear estimation and control. arXiv:2510.22949. https://doi.org/10.48550/arXiv.2510.22949

[23] Cinun, B. C. G., Tamba, T. A., Santjoko, I. R., et al. (2025). Design and experimental validation of closed-form CBF-based safe control for Stewart platform under multiple constraints. arXiv:2512.11125. https://doi.org/10.48550/arXiv.2512.11125

[24] Kazezkhan, G., Xu, Q., Wang, N., et al. (2023). Performance analysis and optimization of a modified Stewart platform for the Qitai radio telescope. Research in Astronomy and Astrophysics, 23(9), 095022. https://doi.org/10.1088/1674-4527/ace1d5

[25] Liang, F., Tan, S., Fan, J., et al. (2021). Design and implementation of a high precision Stewart platform for a space camera. Journal of Physics: Conference Series, 2101, 012015. https://doi.org/10.1088/1742-6596/2101/1/012015

[26] Sun, K., Tang, J., Wu, Z., et al. (2024). Coupled nonlinear vibration characteristics of quasi-zero-stiffness Gough-Stewart isolation platform. Aerospace Science and Technology, 152, 109352. https://doi.org/10.1016/j.ast.2024.109352

[27] Pu, Z. X., Lin, J. H., Guo, J. W., et al. (2025). Performance analysis and optimization of a 6-UPS parallel machine tool. Machine Design and Research, 41(1), 123–127. (In Chinese)

[28] Karmakar, S., & Turner, C. J. (2024). A literature review on Stewart-Gough platform calibrations. Journal of Mechanical Design, 146(8), 050801. https://doi.org/10.1115/1.4064487

[29] Jiang, S. T. (2019). Research on the motion control system of a general aviation flight simulator [Master's thesis]. Hebei University of Science and Technology. (In Chinese)

[30] Yin, D. W., Sun, P., & Zhai, H. Y. (2012). Research on the development of flight simulators and flight simulation training. In Proceedings of the Seventh Jilin Provincial Science and Technology Academic Annual Conference: Innovation-Driven Development and Acceleration of Strategic Emerging Industries (pp. 243–245). Jilin Association for Science and Technology. (In Chinese)

[31] Andrievsky, B., Kazunin, D. V., Kostygova, D. M., et al. (2014). Control of pneumatically actuated 6-DOF Stewart platform for driving simulator. In 2014 19th International Conference on Methods and Models in Automation and Robotics (MMAR) (pp. 663–668). IEEE. https://doi.org/10.1109/MMAR.2014.6957433